EUROPEAN ORGANIZATION FOR NUCLEAR RESEARCH

Proposal to the ISOLDE and Neutron Time-of-Flight Committee

Study of the $N = 28$ shell closure in the argon isotopes

April 9, 2024

A.C. McGlone[1], H.A. Perrett[1], J. Warbinek[2], O. Ahmad[3], S.W. Bai[4], J. Berbalk[3], T.E. Cocolios[3], R.P. de Groote[3], C.M. Fajardo-Zambrano[3], K.T. Flanagan[1], R.F. Garcia Ruiz[5], Á. Koszorús[3,6], L. Lalanne[7], P. Lassegues[3], Y.C. Liu[4], Y.S. Liu[4], K.M. Lynch[1], G. Neyens[3], F. Pastrana[5], J.R. Reilly[2], B. van den Borne[3], R. Van Duyse[3], J. Wessolek[2,1], S.G. Wilkins[5], X.F. Yang[3].

[1] *Department of Physics and Astronomy, The University of Manchester, Manchester, UK*
[2] *Experimental Physics Department, CERN, CH-1211 Geneva 23, Switzerland*
[3] *KU Leuven, Instituut voor Kern- en Stralingsfysica, B-3001 Leuven, Belgium*
[4] *School of Physics and State Key Laboratory of Nuclear Physics and Technology, Peking University, Beijing 100971, China*
[5] *Department of Physics, Massachusetts Institute of Technology, Cambridge, MA 02139, USA*
[6] *Belgian Nuclear Research Centre (SCK CEN), Boeretang 200, 2400, Mol, Belgium*
[7] *IPHC, Université de Strasbourg, Strasbourg F-67037, France*

Spokespersons: A.C. McGlone [abigail.charlotte.mcglone@cern.ch]
H.A. Perrett [holly.perrett@manchester.ac.uk],
J. Warbinek [jessica.warbinek@cern.ch].
Contact persons: J. Warbinek [jessica.warbinek@cern.ch],
A.C. McGlone [abigail.charlotte.mcglone@cern.ch]

CERN-INTC-2024-033 / INTC-P-702
09/04/2024

Abstract: We propose to study the neutron-rich isotopes of Ar ($Z = 18$) around the $N = 28$ shell closure through measuring the spins, nuclear moments and changes in mean-square charge radii for $^{45-48}$Ar. These isotopes lie two protons below the magic Ca nuclei. The moments and spins of ^{45,47}Ar ($N = 27, 29$) will shed light on the persistence of the $N = 28$ shell gap in Ar, investigating the potential onset of deformation along $N = 28$ as protons are removed from the $Z = 20$ shell. Charge radii across $N = 28$ will provide crucial data to study the characteristics of the shell gap in this region.

Requested shifts: 18 shifts with protons (+3 shifts without protons for setup).

1 Physics Motivation

Recent studies of nuclei in the vicinity of $Z = 20$ have focused on the evolution of shell and sub-shell closures for varying Z. A strong shell closure at $N = 28$ for Ca ($Z = 20$) up to Ni ($Z = 28$) isotopes is well documented through studies of the single-particle nature of isotopes along $N = 28$ [1–7]. This is the first shell closure that appears in the shell model due to the contribution of the spin-orbit interaction. Additionally, this region shows evidence of sub-shell gaps at $N = 32, 34$ in the vicinity of $Z = 20$ [8–10]. Experimentally, shell closures are signposted by the disruption of trends in nuclear properties along an isotopic chain, such as the charge radii [11], nuclear moments [12–14], or nuclear masses [15]. A strong shell closure at $N = 28$ is known to exist for the doubly magic ^{48}Ca nucleus, but this devolves to the complete disappearance of the shell closure in ^{42}Si. The disappearance of the $N = 28$ shell closure in Si ($Z = 14$) isotopes has been observed in lifetime measurements [16, 17] and measurements of the first 2^+ excitation energy [18–21]. Erosion of the $N = 28$ shell closure has been shown to already begin in isotopes of S ($Z = 16$). Signatures of shape coexistence in ^{44}S have been observed with a deformed prolate ground state and a quasi-spherical 0^+_2 state [22–24]. Observations of the deformed ^{44}S ground-state strongly mixed with the excited spherical state provide evidence of the breakdown of $N = 28$ in this isotopic chain. This is further supported by shape coexistence seen in ^{43}S [25]. Collective behavior is thought to emerge gradually as the transition occurs from the spherical ^{48}Ca to the deformed ^{42}Si leading to the deformed mixed configuration of ^{44}S [23]. This progressive development of deformation can be described well with Shell-Model calculations using the SPDF-U interaction [3, 26, 27].
Ar ($Z = 18$) lies directly between S and Ca and as such, measurements of Ar will study the progressive erosion of the $N = 28$ shell closure as protons are removed from the $d_{3/2}$ orbital. Existing mass measurements and resulting S_{2n} values indicate a strong shell gap at ^{46}Ar [28], although it was measured as 402(4) keV smaller than the shell gap in ^{48}Ca [15]. However, an elevation in correlation energy in ^{46,47}Ar suggests a description of the Ar ground states that diverges from the expected characteristics of a closed shell nucleus. This implies that the beginnings of collectivity are already appearing within the Ar isotopes [15]. Transfer reactions in ^{47}Ar observed large variations in the f and p spin-orbit splittings which can be accounted for by the proton-neutron tensor force (f) and density dependence (p). This contrasts with previous understandings of the spin-orbit interaction as a purely surface term and can be further investigated with the nuclear moments of Ar isotopes [29]. Additionally, Coulomb excitation measurements [30] show that the shape coexistence in ^{43}S occurs suddenly, with little to no indication in the $N = 27$ isotone of ^{45}Ar. Quadrupole moment predictions using the SPDF-U interaction [31] and low energy Coulomb excitation measurements indicate a prolate shape of the ^{44}Ar nucleus [32]. **Measurements of the nuclear moments of Ar via laser spectroscopy will yield additional information to help improve the description of $N = 28$ shell evolution for different values of Z.**

1.1 Nuclear moments and spin measurements

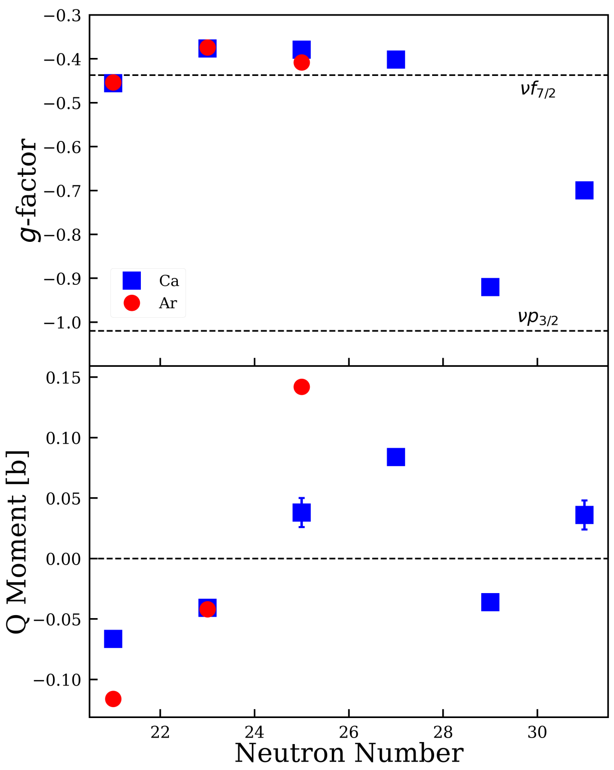

Figure 1: Evolution of measured g-factors and quadrupole moments above $N = 20$ for both Ca [33] and Ar [34].

The magnetic moments of the odd-mass Ar isotopes near $N = 28$ are important for understanding the interplay between many-body correlations and the role of two-body currents in nuclei. The latter has recently been shown to be critical for describing the magnetic moments of medium and heavy mass nuclei, with *ab-inito* theory, without the need of effective operators adjusted to experimental data [35]. In Ref. [34, 36], the magnetic moments of Ar isotopes with unpaired neutrons in the $1\nu f_{7/2}$ shell up to $N = 25$ were shown to agree with effective single-particle values of $g^{\nu} = 0.8g^{\nu}_{free}$. In Figure 1, we plot the experimental g-factors of the odd Ar and Ca isotopes between $N = 20$ and $N = 32$. This observable ($g = \frac{\mu}{I}$) is sensitive to the orbit occupied by the unpaired neutrons [11, 12] irrespective of spin. While all Ca isotopes between $N = 20$ and 28 have a ground-state spin of $I = 7/2$ consistent with an unpaired $\nu f^{-1}_{7/2}$ configuration, the ground-state spins of Ar are more diverse. For ^{39,41}Ar ($N = 21, 23$) the spin is 7/2, but ^{43}Ar ($N = 25$) has a spin 5/2, demonstrating a more complex/mixed wavefunction. However, its g-factor is found similar to that of Ca, which confirms this is a seniority-3 $f_{7/2}$ configuration and highlights the sensitivity of the g-factor to changes in nuclear structure. Its quadrupole moment is also significantly larger than that of the Ca isotone, confirming the seniority-3 configuration. Thus, both the g-factor and quadrupole moment are very sensitive probes to understand the evolution of structure in this region [13]. **In this proposal, we wish to establish the spins (known only tentatively), g-factors and quadrupole moments of ^{45,47}Ar in order to compare these to those of ^{47,49}Ca. This will enable conclusions to be made on the effect that further emptying of the $\pi d_{3/2}$ shell has on the $N = 28$ shell gap.**

Predictions place Ar at the boundary between the magic, spherical behaviour in ^{48}Ca and the onset of shape coexistence in the ground-state of ^{44}S. Calculations using the angular momentum projected generator coordinate method found the shape coexistent ^{44}S ground-state to have an absolute deformation of $|\beta_2|$=0.12 [37]. The predicted deformation for ^{46}Ar amounts to β_2=-0.08, suggesting that shape coexistence decreases in approach of the doubly magic ^{48}Ca [37]. Calculations of quadrupole moments in the $sp - df$ picture confirm this, the quadrupole moments increase considerably with the removal of two or more protons from $Z = 20$ [38]. **Measurements of the quadrupole moments of Ar isotopes will further extend this picture and probe the onset of deformation towards $N = 28$ away from stability.**

1.2 Mapping charge radii

Laser spectroscopy methods have been used to probe the structure of isotopes in the Ca region. A 'kink' in the measured $\delta\langle r^2\rangle$ for isotones of $N = 28$ can be observed consistently in all isotopes from Ni to K (see Figure 2) [11]. This change in the gradient of $\delta\langle r^2\rangle$ is a signature typically observed at a spherical shell closure [39], thus indicating the strength of the $N = 28$ shell gap around $Z = 20$. Beyond the $N = 28$ shell closure, the measured $\delta\langle r^2\rangle$ for isotopes between $Z = 20$ and $Z = 28$ increase steeply and monotonically up to $N = 32$ with similar rates [40–43]. The K [41], Mn [42], Fe [43], and Ni [7] isotopic chains exhibit no observable $N = 32$ closure in the charge radii (Figure 2). It was suggested in Ref.[44] that an effective increase in size of shell-model valence p-wave neutron orbitals, influencing the proton radial extension, explains the observed increase of charge radius in Ca isotopes while maintaining the doubly-magic character of ^{52}Ca. This was experimentally confirmed in Ref. [45] through a neutron-knockout reaction study. The charge radii of Ar isotopes are currently limited to $N = 28$ [34, 36] but are missing ^{45}Ar. **Systematic measurements of the radii of Ar isotopes past $N = 28$ would provide additional information on the behaviour of the $N = 28$ shell gap and the onset of collectivity between Ca and S.**

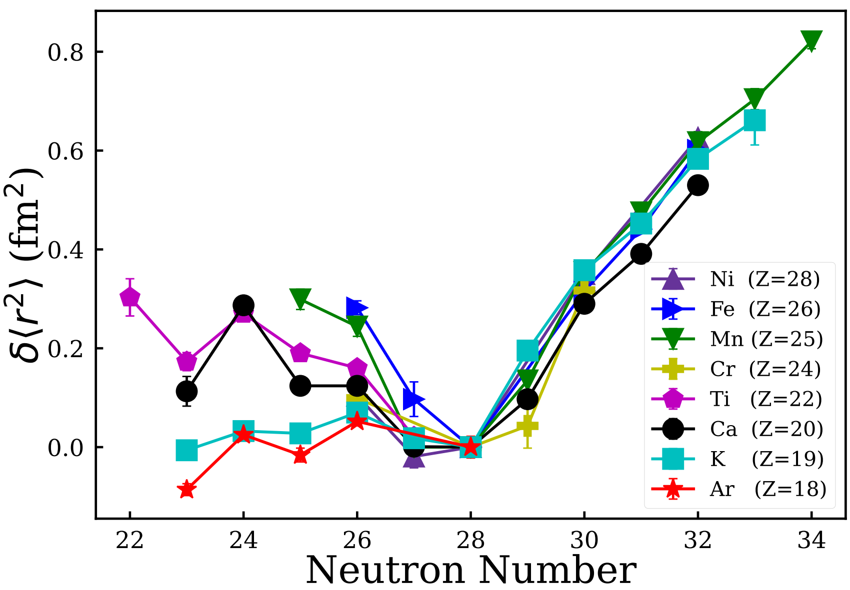

Figure 2: The measured trend in mean-square charge radii for Ar [34, 36] and regional systematics around $N = 28$ [7, 41].

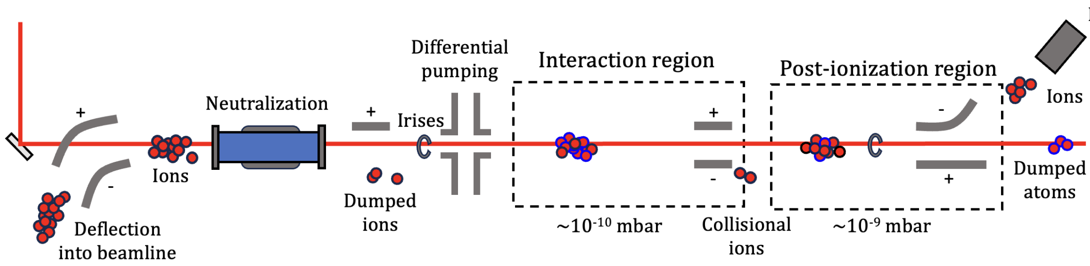

Figure 3: Schematic diagram of the CRIS experiment that will be used to measure the neutron-rich Ar isotopes.

2 Experimental Details

The Collinear Resonance Ionization Spectroscopy (CRIS) experiment will be used to measure the hyperfine structure and isotope shifts of the neutron-rich Ar isotopes. This combines the high resolution of the collinear-beam method with the high sensitivity of RIS to measure elements with low production yields [46, 47]. We propose to use a uranium carbide (UC_x) target and cold plasma ion source. The resultant beam will be separated using the high-resolution separator, HRS, bunched using ISCOOL, and then deflected into the CRIS beamline, schematically presented in Figure 3. The bunched ion beam will undergo neutralisation with K vapour inside the CRIS charge-exchange cell. Post charge-exchange, 40% of the Ar atoms will be in the $4s[3/2]_2$ metastable state for a 40-keV beam [36, 48]. Any residual ions post-neutralisation will be separated from the atomic beam before it enters the interaction region, where it is overlapped spatially and temporally with pulsed lasers. The resonantly-produced ions are then deflected by a 34°-bender and detected using either a MagneTOF detector or a decay spectroscopy station.

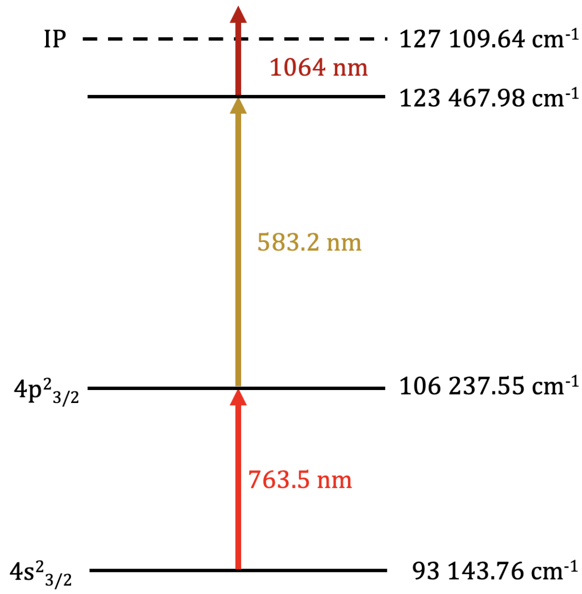

Figure 4: Three step resonant ionization scheme for Ar. First step transition has been previously used by [34].

An illustration of the three-step ionization scheme can be found in Figure 4. The first step of the RIS scheme will use the $4s[3/2]_2 \rightarrow 4p[3/2]_2$ transition, which has previously been used to successfully measure nuclear moments and isotope shifts [34, 36]. A three-step RIS scheme will be used and can be produced with the available lasers at CRIS. The required three-step scheme relies on fundamental wavelengths, and as such will have sufficient power for the required transitions. The first step will be produced with a narrowband injection-seeded Ti:Sa cavity, which has a linewidth of ∼20 MHz [49]. A Pulsed Dye Laser (PDL) using Pyrromethene dye to produce 583.2 nm light will provide the second step. This will allow the atoms to be photoionized by a 1064 nm non-resonant step. The choice of a resonance scheme with a non-resonant laser step of 1064 nm in comparison to lower wavelengths will reduce the laser-induced background of our measurements. In addition to this, production of collisional ions through interactions of neutral atoms after the charge exchange process is reduced by the ultra-high vacuum achieved within the interaction region of the CRIS beamline. The interaction region is routinely operated with an ultra-high vacuum of 10^{-10} mbar. The beam time estimates have been made based on previous signal-to-noise measurements with the CRIS experiment and a 40% neutralization efficiency from previous fast-beam laser spectroscopy measurements at ISOLDE [36].

3 Beam Time Request

Isotope	$T_{1/2}$	I^{π}	Yield (/μC	Shifts Required	Measurements
$^{38-44}$Ar	stable-8s	–	10^6-10^7*	3	Reference μ, Q and $\delta\langle r^2\rangle$
^{45}Ar	21.48(15) s	(5/2,7/2)	3.49×10^5*	2	I, μ, Q and $\delta\langle r^2\rangle$
^{46}Ar	8.4 s	0^+	1.11×10^5*	2	Reference $\delta\langle r^2\rangle$
^{47}Ar	1.23(3) s	$(3/2^-)$	7.72×10^3*	6	I, μ, Q and $\delta\langle r^2\rangle$
^{48}Ar	415(15) ms	0^+	1.58×10^3*	5	$\delta\langle r^2\rangle$

Table 1: Isotopes of interest, half-lives, measured and expected yields, number of shifts requested with a UCx target and protons on target. Yields with a * represent predicted values extrapolated from existing yield measurements and Ar half-lives with thanks to the Targets Team.

In total we request **18 shifts** with protons using a **UCx** target and a low temperature, water-cooled transfer line to a FEBIAD-type plasma ion-source. By maintaining a low temperature on the transfer line, only species that are gaseous at room temperature will be ionized reducing isobaric contamination. The beams of Ar will be contaminated with Kr^{2+} and Xe^{3+}, by a factor of approximately 100 from ^{45}Ar to ^{48}Ar. In addition to this, a large volume of stable contamination is expected. The CRIS technique has previously measured cases where the isobar has been produced with 4 orders of magnitude higher intensity. The beam time request has been estimated using the required shifts to measure ^{78}Cu [46], ^{52}K [41] and ^{131}In [47] with CRIS, considering the expected background rates and RIS efficiency. The shift request accounts for a reduced yield for all isotopes due to a short beam gate and frequency scanning synchronised with one step per super cycle to reduce the effects of isobaric contamination.
The requested shifts for ^{48}Ar accounts for the lack of hyperfine structure (a single resonance requires a smaller scanning region), the stable molecule contamination and reduced contamination from 2+ and 3+ species. In order to account for the voltage calibration

of ISCOOL and other systematic effects, a total of **5 shifts** are required for reference measurements across the previously-measured isotopes $^{38-44,46}$Ar. Additionally, **3 shifts** without protons are requested to optimize the CRIS setup with stable Ar beams from the plasma ion source. This is essential to optimize the neutralization process and laser-atom overlap to maximise the sensitivity to the most radioactive cases.

References

[1] F Sarazin et al. Shape coexistence and the $N = 28$ shell closure far from stability. Phys. Rev. Lett., 84:5062–5065, May 2000.

[2] E Caurier, F Nowacki, and A Poves. The $N = 28$ shell closure; from $N = Z$ to the neutron drip line. Nuclear Physics A, 742(1):14–26, 2004.

[3] L Gaudefroy. Shell model study of $N \simeq 28$ neutron-rich nuclei. Phys. Rev. C, 81:064329, June 2010.

[4] O Sorlin and M-G Porquet. Evolution of the $N = 28$ shell closure: a test bench for nuclear forces. Physica Scripta, 2013(T152):014003, January 2012.

[5] X-W Xia. Evolution of $N = 28$ shell closure in relativistic continuum Hartree-Bogoliubov theory. Chinese Physics C, 40(7):074101, July 2016.

[6] S W Bai et al. Electromagnetic moments of scandium isotopes and N=28 isotones in the distinctive $0f_{7/2}$ orbit. Physics Letters B, 829:137064, 2002.

[7] F Sommer et al. Charge radii of ^{55,56}Ni reveal a surprisingly similar behavior at $N = 28$ in Ca and Ni isotopes. Phys. Rev. Lett., 129:132501, Sep 2022.

[8] F Wienholtz et al. Masses of exotic calcium isotopes pin down nuclear forces. Nature, 498:346–9, 06 2013.

[9] J I Prisciandaro, P F Mantica, et al. New evidence for a subshell gap at $N = 32$. Physics Letters B, 510(1):17–23, 2001.

[10] T Otsuka, A Gade, O Sorlin, T Suzuki, and Y Utsuno. Evolution of shell structure in exotic nuclei. Review of Modern Physics, 92:015002, March 2020.

[11] I Angeli and K P Marinova. Correlations of nuclear charge radii with other nuclear observables. Journal of Physics G: Nuclear and Particle Physics, 42(5):055108, 2015.

[12] G Neyens. Nuclear magnetic and quadrupole moments for nuclear structure research on exotic nuclei. Reports on Progress in Physics, 66:633, 2003.

[13] R P de Groote and G Neyens. Spins and electromagnetic moments of nuclei. Handbook of Nuclear Physics, I. Tanihata et al. (eds.), 2023.

[14] X Yang, S Wang, S Wilkins, and R Garcia Ruiz. Laser spectroscopy for the study of exotic nuclei. Progress in Particle and Nuclear Physics, 129:104005, 2023.

[15] M Mougeot et al. Examining the $N = 28$ shell closure through high-precision mass measurements of $^{46-48}Ar$. Physical Review C, 102:014301, July 2020.

[16] S Grévy et al. Beta-decay studies at the $N = 28$ shell closure. Nuclear Physics A, 722:C424–C428, July 2003.

[17] H L Crawford et al. Crossing $N = 28$ toward the neutron drip line: First measurement of half-lives at frib. Phys. Rev. Lett., 129:212501, November 2022.

[18] B Bastin et al. Collapse of the $N = 28$ Shell Closure in ^{42}Si. Phys. Rev. Lett., 99(2):022503, July 2007. Publisher: American Physical Society.

[19] C M Campbell et al. Measurement of Excited States in ^{40}Si and Evidence for Weakening of the $N = 28$ Shell Gap. Phys. Rev. Lett., 97(11):112501, September 2006.

[20] S Takeuchi et al. Well Developed Deformation in ^{42}Si. Phys. Rev. Lett., 109(18):182501, November 2012. Publisher: American Physical Society.

[21] A Gade et al. Is the Structure of ^{42}Si Understood? Phys. Rev. Lett., 122(22):222501, June 2019. Publisher: American Physical Society.

[22] T Glasmacher et al. Collectivity in ^{44}S. Physics Letters B, 395(3):163–168, March 1997.

[23] C Force et al. Prolate-Spherical Shape Coexistence at $N = 28$ in ^{44}S. Phys. Rev. Lett., 105(10):102501, September 2010.

[24] D Santiago-Gonzalez et al. Triple configuration coexistence in ^{44}S. Phys. Rev. C, 83(6):061305, June 2011.

[25] L Gaudefroy et al. Shell Erosion and Shape Coexistence in $^{43}_{16}S_{27}$. Phys. Rev. Lett., 102(9):092501, March 2009. Publisher: American Physical Society.

[26] S Bhattacharyya et al. Structure of neutron-rich ar isotopes beyond $N = 28$. Phys. Rev. Lett., 101:032501, July 2008.

[27] F Nowacki and A Poves. New effective interaction for $0\hbar\omega$ shell-model calculations in the $sd-pf$ valence space. Phys. Rev. C, 79:014310, January 2009.

[28] Z Meisel et al. Mass measurements demonstrate a strong $N = 28$ shell gap in argon. Phys. Rev. Lett., 114:022501, January 2015.

[29] L Gaudefroy et al. Reduction of the spin-orbit splittings at the $N = 28$ shell closure. Phys. Rev. Lett., 97:092501, August 2006.

[30] B Longfellow et al. Shape changes in the $N = 28$ island of inversion: Collective structures built on configuration-coexisting states in ^{43}S. Phys. Rev. Lett., 125:232501, December 2020.

[31] Y Utsuno, T Otsuka, B A Brown, M Honma, T Mizusaki, and N Shimizu. Shape transitions in exotic Si and S isotopes and tensor-force-driven Jahn-Teller effect. Physical Review C, 86:051301, November 2012.

[32] M Zielińska et al. Shape of ^{44}Ar: Onset of deformation in neutron-rich nuclei near ^{48}Ca. Phys. Rev. C, 80:014317, July 2009.

[33] R F Garcia Ruiz et al. Ground-state electromagnetic moments of calcium isotopes. Physical Review C, 91:041304, 2015.

[34] K Blaum, W Geithner, J Lassen, P Lievens, K Marinova, and R Neugart. Nuclear moments and charge radii of argon isotopes between the neutron-shell closures $N = 20$ and $N = 28$. Nuclear Physics A, 799(1):30–45, 2008.

[35] T Miyagi et al. Impact of two-body currents on magnetic dipole moments of nuclei. Arxiv, page arXiv:2311.14383, December 2023.

[36] A Klein, B A Brown, U Georg, M Keim, P Lievens, R Neugart, M Neuroth, R E Silverans, L Vermeeren, and ISOLDE Collaboration. Moments and mean square charge radii of short-lived argon isotopes. Nuclear Physics A, 607(1):1–22, 1996.

[37] R Rodríguez-Guzmán, J L Egido, and L M Robledo. Quadrupole collectivity in $N \approx 28$ nuclei with the angular momentum projected generator coordinate method. Phys. Rev. C, 65:024304, January 2002.

[38] R A Radhi et al. Magnetic dipole moments, electric quadrupole moments, and electron scattering form factors of neutron-rich $sd-pf$ cross-shell nuclei. Phys. Rev. C, 97:064312, June 2018.

[39] X Yang et al. Precision laser spectroscopy technique for exotic radioactive beams at CERN-ISOLDE. Journal of Physics: Conference Series, 1024(1):012031, May 2018.

[40] R Garcia Ruiz et al. Unexpectedly large charge radii of neutron-rich calcium isotopes. Nature Physics, 12:594, February 2016.

[41] Á Koszorús, X Yang, et al. Charge radii of exotic potassium isotopes challenge nuclear theory and the magic character of $N = 32$. Nature Physics, 17:1–5, April 2021.

[42] H Heylen et al. Changes in nuclear structure along the mn isotopic chain studied via charge radii. Physical Review C, 94, September 2016.

[43] K Minamisono et al. Charge radii of neutron deficient ^{52,53}Fe produced by projectile fragmentation. Physical Review Letters, 117:252501, December 2016.

[44] J Bonnard, S M Lenzi, and A P Zuker. Neutron skins and halo orbits in the sd and pf shells. Phys. Rev. Lett., 116:212501, May 2016.

[45] M Enciu et al. Extended $p_{3/2}$ neutron orbital and the $N = 32$ shell closure in ^{52}Ca. Physical Review Letters, 129:262501, December 2022.

[46] R P de Groote et al. Measurement and microscopic description of odd–even staggering of charge radii of exotic copper isotopes. Nature Physics, 16(6):620–624, 2020.

[47] A R Vernon, R F Garcia Ruiz, T Miyagi, et al. Nuclear moments of indium isotopes reveal abrupt change at magic number 82. Nature, 607(7918):260–265, 2022.

[48] A R Vernon et al. Simulation of the relative atomic populations of elements $1 \leq Z \leq 89$ following charge exchange tested with collinear resonance ionization spectroscopy of indium. Spectrochimica Acta Part B: Atomic Spectroscopy, 153:61–83, 2019.

[49] V Sonnenschein et al. Characterization of a pulsed injection-locked Ti:sapphire laser and its application to high resolution resonance ionization spectroscopy of copper. Laser Physics, 27(8):085701, July 2017.

4 Details for the Technical Advisory Committee

4.1 General information

Describe the setup which will be used for the measurement. If necessary, copy the list for each setup used.

☒ Permanent ISOLDE setup: CRIS

☒ To be used without any modification

4.2 Beam production

- Requested beams:

Isotope	Production yield in focal point of the separator (/μC)	Minimum required rate at experiment (pps)	$t_{1/2}$
$^{38-44}$Ar	10^6-10^7*	10^6	stable -8s
^{45}Ar	3.49×10^5*	10^4	21.48(15) s
^{46}Ar	1.11×10^5*	10^3	8.4 s
^{47}Ar	7.72×10^3*	10^3	1.23(3) s
^{48}Ar	1.58×10^3*	10^3	415(15) ms

- Full reference of yield information: ISOLDE Yield Database, ISOLTRAP [15], COLLAPS[34]. Yields with a * represent predicted values extrapolated from existing yield measurements and Ar half-lives with thanks to the Targets Team. Minimum required rate at experiment accounts for the short beamgate and synchronisation with the proton supercycle that will be used to limit contamination.

- Target - ion source combination: UCx target and a low temperature, water-cooled transfer line to a FEBIAD-type plasma ion-source.

- RILIS? NO.

- Additional features? NO.

- Expected contaminants: We expect contamination from Kr^{2+} and Xe^{3+}. Additional stable contaminants were observed by ISOLTRAP in [15] such as the stable $^{34}S^{12}C^+$ or $^{34}S^{12}C^+$ molecular ions.

- Acceptable level of contaminants: Contamination level will be limited using a short beamgate, synchronised witht the proton supercycle to only allow for data taking after a proton pulse.

- Can the experiment accept molecular beams: NO.

- Are there any potential synergies (same element/isotope) with other proposals and LOIs that you are aware of? NO.

4.3 Shift breakdown

Summary of requested shifts:

With protons	Requested shifts
Reference measurements and data taking $^{38-44}$Ar	3
Data taking, ^{45}Ar	2
Data taking, ^{46}Ar	2
Data taking, ^{47}Ar	6
Data taking, ^{48}Ar	5
Without protons	Requested shifts
Stable beam for CRIS setup and optimization	3

4.4 Health, Safety and Environmental aspects

4.4.1 Radiation Protection

- If radioactive sources are required: N/A
- For collections: N/A